



Short communication

Hydrogenation of CO₂ to dimethyl ether on La-, Ce-modified Cu-Fe/HZSM-5 catalysts

Zu-zeng Qin^{a,*}, Xin-hui Zhou^a, Tong-ming Su^a, Yue-xiu Jiang^a, Hong-bing Ji^{a,b,**}^a School of Chemistry and Chemical Engineering, Guangxi Key Laboratory of Petrochemical Resource Processing and Process Intensification Technology, Guangxi University, Nanning 530004, PR China^b School of Chemistry and Chemical Engineering, Sun Yat-sen University, Guangzhou 510275, PR China

ARTICLE INFO

Article history:

Received 19 October 2015

Received in revised form 4 December 2015

Accepted 12 December 2015

Available online 13 December 2015

Keywords:

CO₂ hydrogenation

Cu based catalysts

DME synthesis

Mixed oxide

Bifunctional catalyst

ABSTRACT

Cu–Fe–La/HZSM-5 and Cu–Fe–Ce/HZSM-5 bifunctional catalysts were prepared and applied for the direct synthesis of dimethyl ether (DME) from CO₂ and H₂. The catalysts were characterized by X-ray diffraction (XRD), N₂ adsorption–desorption, H₂-temperature programmed reduction (H₂-TPR), and X-ray photoelectron spectroscopy (XPS). The results showed that La and Ce significantly decreased the outer-shell electron density of Cu and improved the reduction ability of the Cu–Fe catalyst in comparison to the Cu–Fe–Zr catalyst, which may increase the selectivity for DME. The Cu–Fe–Ce catalyst had a greater specific surface area than the Cu–Fe–La catalyst. This promoted CuO dispersion and decreased CuO crystallite size, which increased both the DME selectivity and the CO₂ conversion. The catalysts were stable for 15 h.

© 2015 Elsevier B.V. All rights reserved.

1. Introduction

With the economic development and the expansion of industrialization, the combustion of coal, gasoline, natural gas, and other hydrocarbons increases the CO₂ content in the atmosphere every year, causing the earth's temperature to rise [1]. However, CO₂ is also a potential carbon resource. To utilize CO₂ and solve the environmental problems caused by CO₂, the key issue is to develop technologies to capture, store and use CO₂ [2,3]. One way to do this is to effectively translate CO₂ into hydrocarbon fuels by, for example, CO₂ hydrogenation to dimethyl ether (DME) [4].

Presently, there are two main processes for synthesizing DME — a two-step process and a one-step process — using CO₂ and H₂ as the raw materials. The one-step process combines methanol synthesis and methanol dehydration catalysts in the same reactor to directly synthesize DME from CO₂ and H₂. This method has received considerable attention, as it is thermodynamically and economically more advantageous than the traditional two-step process. However, the one-step process still remains in the laboratory exploration stage. The catalysts used in the one-step process to synthesize DME include Cu-based catalysts such as CuO–TiO₂–ZrO₂/HZSM-5 [5], Cu–ZnO/Al₂O₃ [6], CuO–ZnO–

Al₂O₃/HZSM-5 [7,8], CuO–ZnO–Al₂O₃–ZrO₂/HZSM-5 [9], and Cu–ZnO–ZrO₂/HZSM-5 [10], along with non-Cu-based catalysts including Pd–Pd₂Ga [11,12]. Due to the stability of CO₂, its activation is a bottleneck problem that is difficult to solve, and the CO₂ hydrogenation reaction is conducted at 4–8 MPa and 250–350 °C, leading to the deactivation of the catalyst. Even when used Cu–Fe–Zr/HZSM-5 was used as catalyst [13,14], which decreased the pressure and temperature to 3–4 MPa and 220–260 °C, respectively, the conversion of CO₂ was still only 25%–30% and the selectivity of DME was only 40%–50% [13,15], limiting the industrial application of this method.

La and Ce have been added to catalysts to promote the dispersion of metal, decrease the reduction temperature and the crystallite size, and improve the thermal stability of the catalyst [16–18]. Based on a previous Cu–Fe–Zr catalyst [13,14], the Cu–Fe–La, and Cu–Fe–Ce catalysts were synthesized in this work using a homogeneous precipitation method. The catalysts were then characterized by X-ray diffractometer (XRD), N₂ adsorption–desorption, H₂-temperature programmed reduction (H₂-TPR), and X-ray photoelectron spectrometer (XPS), and applied in the hydrogenation of CO₂ to DME.

2. Experimental

2.1. Preparation of catalyst

The precursor of the methanol synthesis catalyst was prepared by homogeneous precipitation. Cu(NO₃)₂·3H₂O and Fe(NO₃)₃·9H₂O were weighed according to the Cu/Fe molar ratio of 3:2. Likewise,

* Correspondence to: Z.-z Qin, School of Chemistry and Chemical Engineering, Guangxi University, Nanning 530004, PR China.

** Correspondence to: H.-b Ji, School of Chemistry and Chemical Engineering, Sun Yat-sen University, Guangzhou 510275, PR China.

E-mail addresses: qinzuzeng@gmail.com (Z. Qin), jihb@mail.sysu.edu.cn (H. Ji).

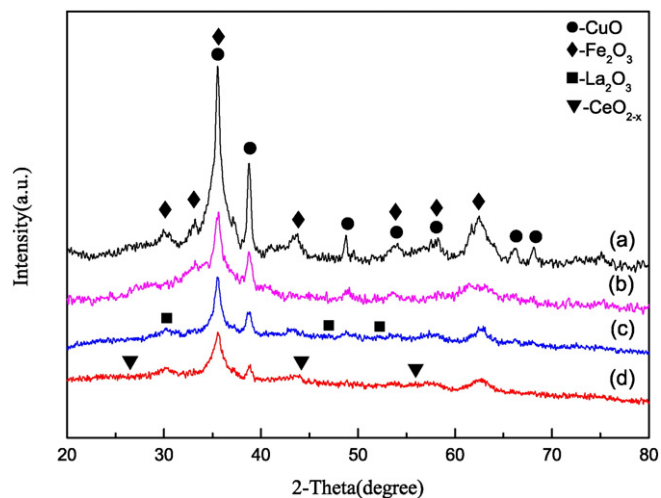


Fig. 1. XRD patterns of Cu-Fe (a), Cu-Fe-Zr (b), Cu-Fe-La (c) and Cu-Fe-Ce (d) calcined at 400 °C without H₂ reduction.

Zr(NO₃)₄·5H₂O, La(NO₃)₃·6H₂O, and Ce(NO₃)₃·6H₂O were weighed based on the corresponding ZrO₂, La₂O₃, and CeO₂ contents of 1.0 wt% in the ternary metal oxides. After mixed oxide Cu-Fe-Ce, Cu-Fe-La and Cu-Fe-Zr (i.e., the methanol dehydration components) were prepared via homogeneous precipitation, they were mechanically mixed with HZSM-5 (Shanghai Novel Chemical Technology Co., Ltd.) with a silica–alumina ratio of 300:1 in a 1:1 mass ratio. The details of the preparation method are given in the supporting information.

2.2. Characterization of the catalyst

XRD, XPS, N₂ adsorption–desorption and H₂-TPR were used to characterize the catalysts following previously reported procedures [13].

2.3. Catalytic hydrogenation of CO₂ to DME

The reaction process for DME synthesis from CO₂ and H₂ can be found in the literature [13]. The feed gas was a mixture of H₂ and CO₂ gas (4:1 mol ratio) after reduction, and the catalytic hydrogenation of CO₂ to DME was performed at 260 °C and 3.0 MPa with a gaseous hourly space velocity (GHSV) of 1500 mL·g_{cat}⁻¹·h⁻¹. The details of the catalytic hydrogenation of CO₂ to DME are found in the literature [13].

3. Results and discussion

3.1. XRD analysis

Fig. 1 shows the XRD patterns of the Cu-Fe, Cu-Fe-Zr, Cu-Fe-La and Cu-Fe-Ce catalysts calcined at 400 °C without H₂ reduction.

The characteristic peaks of monoclinic CuO (JCPDS No. 48-1548) at $2\theta = 35.49^\circ$, 38.69° , and 58.26° and of cubic crystalline Fe₂O₃ (JCPDS No. 39-1346) at $2\theta = 30.24^\circ$, 35.63° , and 62.93° are found in the XRD patterns of Cu-Fe-La and Cu-Fe-Ce. Compared with Cu-Fe and Cu-Fe-Zr, the diffraction peaks of CuO and Fe₂O₃ in the Cu-Fe-La and Cu-Fe-Ce patterns are broadened, and the peak intensities are weakened, indicating that the crystallite size of CuO is smaller. Smaller crystallites correspond to better copper dispersion. The crystallite sizes of CuO (111) in the Cu-Fe-La and Cu-Fe-Ce catalysts were calculated using the Sherrer equation and determined to be 19.1 and 17.6 nm, respectively. However, the crystallite sizes in the Cu-Fe and Cu-Fe-Zr catalysts are 22.5 and 19.3 nm, respectively, indicating that the modification of La₂O₃ and CeO₂ decreased the crystallite size of CuO and promoted the dispersion of CuO [19]. The crystallite size of the Cu-Fe-Ce catalyst is clearly the smallest among the catalysts. The diffraction peaks at $2\theta = 29.9^\circ$, 46.1° , and 52.1° were attributed to the La₂O₃ phase (JCPDS No. 05-0602). Peaks corresponding to CeO_{2-x} at $2\theta = 26.3^\circ$, 43.9° and 55.7° (JCPDS No. 49-1415) were found. These results suggested that some of the smaller-sized Cu²⁺ ions (ionic radius of 0.79 Å compared to 0.92 Å for Ce⁴⁺) entered the CeO₂ lattice to form a Ce_{1-x}Cu_xO_{2-x} solid solution [20].

3.2. Nitrogen adsorption/desorption of catalysts

Fig. 2 shows the N₂ adsorption–desorption isotherms and pore size distribution profiles of the Cu-Fe, Cu-Fe-Zr, Cu-Fe-La, and Cu-Fe-Ce catalysts calcined at 400 °C without H₂ reduction.

Based on the IUPAC classification, the N₂ adsorption–desorption isotherms of the Cu-Fe-La and Cu-Fe-Ce catalysts (Fig. 2A) belonged to IV-type isotherms. In the low- and medium-pressure region ($P/P_0 = 0.0$ – 0.8), the amount of adsorbed N₂ gently increased, indicating that the adsorption of N₂ on the internal surfaces of catalyst pores shifted from monolayer to multilayer. In the high-pressure region ($P/P_0 = 0.8$ – 1.0), an H3-type hysteresis loop was generated by capillary condensation, suggesting that the Cu-Fe-La and Cu-Fe-Ce catalysts were mesostructured materials [21]. The pore size distribution profiles (Fig. 2B) indicate that the majority of mesopores had diameters of approximately 3 nm. The specific surface areas of the Cu-Fe, Cu-Fe-Zr, Cu-Fe-La, and Cu-Fe-Ce catalysts were calculated using the Brunauer–Emmett–Teller (BET) equation according to the N₂

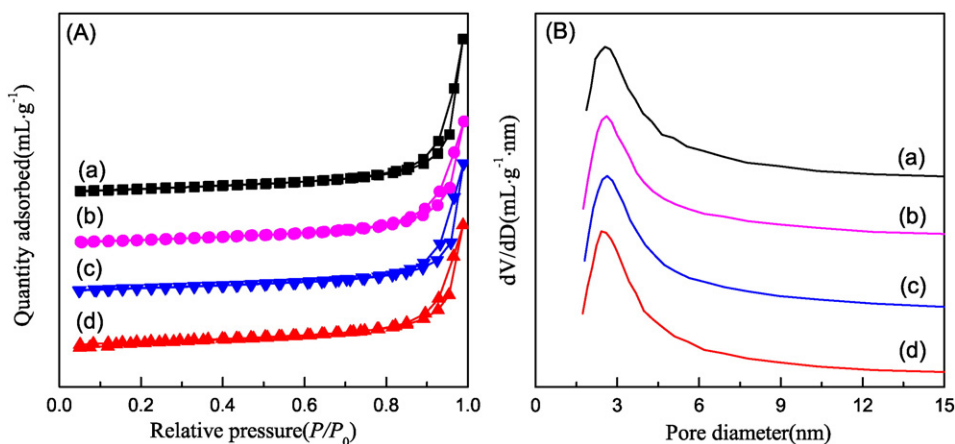


Fig. 2. Nitrogen adsorption/desorption isotherms (A) and pore size distribution profiles (B) of Cu-Fe (a), Cu-Fe-Zr (b), Cu-Fe-La (c) and Cu-Fe-Ce (d) catalysts calcined at 400 °C without H₂ reduction.

Table 1
Textural properties of Cu-Fe, Cu-Fe-Zr, Cu-Fe-La and Cu-Fe-Ce catalysts.

Catalyst	BET surface area ($\text{m}^2 \cdot \text{g}^{-1}$)	Average pore diameter (nm)
Cu-Fe	50.32	25.54
Cu-Fe-Zr	52.37	20.86
Cu-Fe-La	52.55	23.44
Cu-Fe-Ce	56.41	20.62

adsorption isotherms, and the results are shown in Table 1. The specific surface areas of the Cu-Fe, Cu-Fe-Zr, Cu-Fe-La and Cu-Fe-Ce catalysts were 50.32, 52.37, 52.55, and 56.41 $\text{m}^2 \cdot \text{g}^{-1}$, respectively. Based on the 4f electron orbit and structural relaxation of Ce, the CeO particle size will be reduced, consequently increasing the surface area and the concentration of defects, such as oxygen vacancies [22]. Similar results were obtained after modification with La and Zr.

3.3. Results of X-ray photoelectron spectroscopy

XPS was applied to study the oxidation states of the elements on the surfaces of the Cu-Fe, Cu-Fe-Zr, Cu-Fe-La, and Cu-Fe-Ce catalysts (Fig. 3).

In Fig. 3, the binding energy of Cu $2p_{3/2}$ in the Cu-Fe-Ce catalyst was 933.97 eV, with featured satellite peaks at approximately 941.37 eV. The binding energy of Cu $2p_{1/2}$ was 953.97 eV, with featured satellite peaks at approximately 962.42 eV. Likewise, the binding energy of Cu $2p_{3/2}$ in the Cu-Fe-La catalyst was 933.77 eV, with featured satellite peaks at approximately 941.57 eV, and the binding energy of Cu $2p_{1/2}$ was 953.82 eV, with featured satellite peaks at approximately 962.52 eV. Hence, it can be determined that Cu occurred in the form of Cu^{2+} in CuO [23]. After modification with Zr, La, and Ce, XPS analysis showed that the Cu $2p_{3/2}$ and Cu $2p_{1/2}$ major peaks shifted by 0.18 and 0.31 eV [13], 0.17 and 0.37 eV, and 0.37 and 0.52 eV, respectively, towards higher binding energies. These data suggest that Zr, La, and Ce can exchange electrons with CuO, decreasing the outer-shell electron density of Cu and slightly affecting the chemical combination state of CuO [24], finally influencing the catalytic activities of the catalysts. Furthermore, after modification with Ce, the binding energies of Cu $2p_{3/2}$ and Cu $2p_{1/2}$ show a maximum red shift among the three kinds of modifiers,

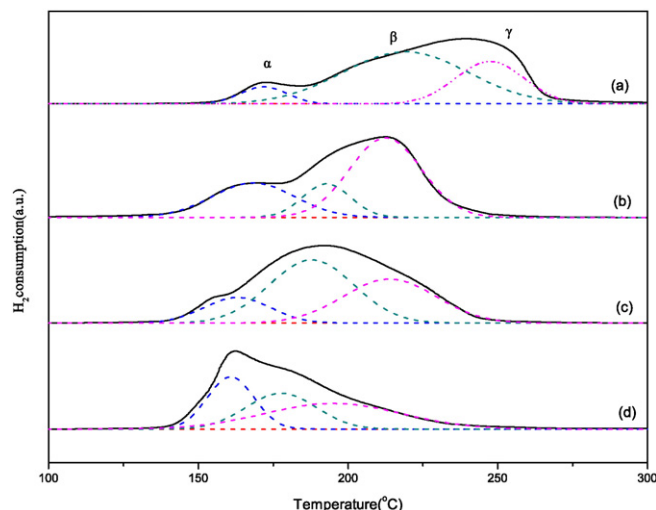


Fig. 4. H_2 -TPR profiles for Cu-Fe, Cu-Fe-Zr, Cu-Fe-La and Cu-Fe-Ce catalysts. The solid curves are experimental curves, and broken curves are Gaussian multipeak fitting curves.

indicating that Ce modification has the greatest effect on the outer electron density of Cu. Considering the XRD results, this likely occurs because CuO and CeO_2 form a solid solution.

In Fig. 3, the binding energies of Fe $2p_{3/2}$ and Fe $2p_{1/2}$ in the Cu-Fe-La and Cu-Fe-Ce catalysts were 711.07 eV and 724.62 eV, and 711.17 eV and 724.47 eV, respectively, suggesting that the chemical valence of Fe was Fe^{3+} in Fe_2O_3 [25]. Seven peaks can be fit in the XPS spectrum of La 3d in the Cu-Fe-La catalyst; the solid curves correspond to La $3d_{5/2}$ and the broken curves correspond to La $3d_{3/2}$, suggesting that the chemical valence of La was La^{3+} [26]. Fig. 3 shows the XPS spectrum of Ce 3d in the Cu-Fe-Ce catalyst. Due to the hybridization between Ce 4f and O 2p, the explanation of Ce 3d was more complex [27]. Two sets of spin-orbit multiplets were observed: U and V correspond to Ce $3d_{3/2}$ and Ce $3d_{5/2}$ contributions, respectively. The Ce 3d spectrum contains three main Ce $3d_{5/2}$ features at 883.1 (V_1), 889.5 (V_2), and 898.5 (V_3) eV and three main Ce $3d_{3/2}$ features at 902.6 (U_1), 912.3 (U_2), and 917.1 (U_3) eV, indicating that Ce exists in Cu-Fe-Ce catalyst as Ce^{3+} and Ce^{4+} [28–30].

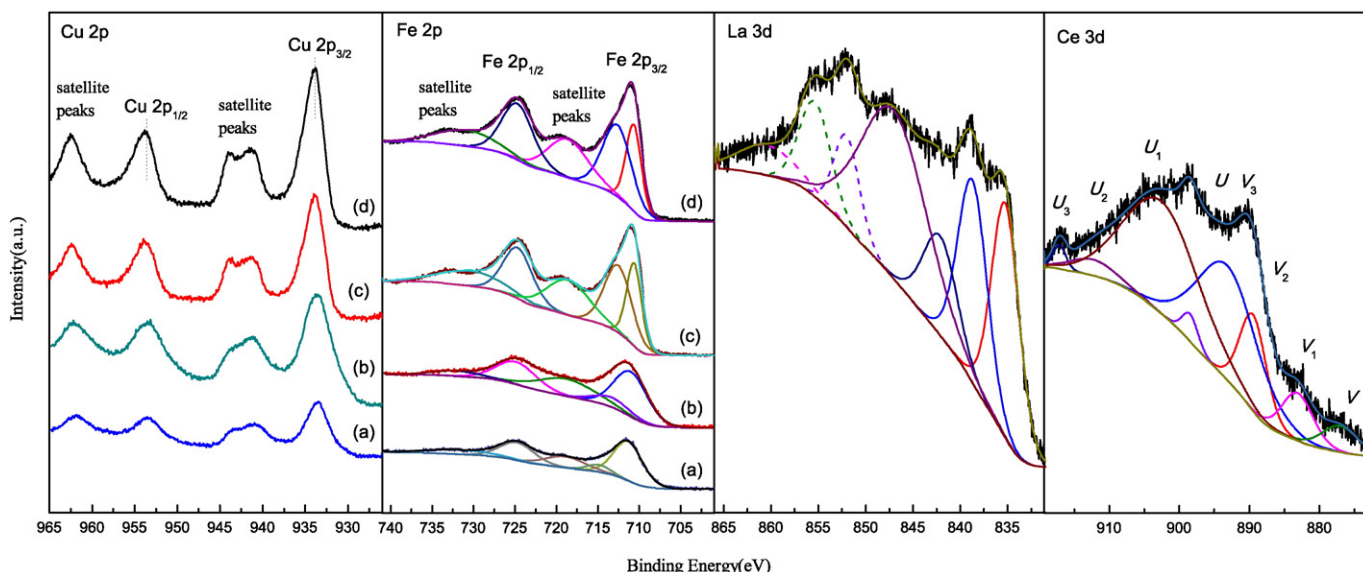


Fig. 3. XPS spectra of Cu 2p, Fe 2p, La 3d and Ce 3d regions for Cu-Fe (a), Cu-Fe-Zr (b), Cu-Fe-La (c) and Cu-Fe-Ce (d) catalysts.

Table 2

Temperatures and areas of the reduction peaks of Cu–Fe, Cu–Fe–Zr, Cu–Fe–La, and Cu–Fe–Ce catalysts.^a

Catalyst	Peak α		Peak β		Peak γ		Total area
	T (°C)	Area ^b	T (°C)	Area	T (°C)	Area	
Cu–Fe	172	0.89	219	7.30	247	3.26	11.45
Cu–Fe–Zr	168	3.33	193	1.89	213	6.78	11.97
Cu–Fe–La	161	1.91	182	5.98	209	4.57	12.46
Cu–Fe–Ce	156	2.31	178	2.39	195	3.34	8.04

^a The results were measured from H₂-TPR profiles, and the areas were calculated by integrating the areas under the peaks.

^b The unit of peak area is $\times 10^4$ units.

Table 3

DME synthesis by CO₂ hydrogenation over Cu–Fe based catalysts.^a

Catalyst	Conversion of CO ₂ (mol%)	Selectivity of products (mol%)				Yield of DME (mol%)
		DME	CH ₃ OH	CO	CH ₄	
Cu–Fe/HZSM-5	12.3	18.3	0.9	30.5	50.3	2.3
Cu–Fe–Zr/HZSM-5	17.3	39.9	1.9	21.3	36.9	6.9
Cu–Fe–La/HZSM-5	17.2	51.3	1.5	30.3	16.9	8.8
Cu–Fe–Ce/HZSM-5	18.1	52.0	2.1	25.4	20.5	9.4

^a Reaction conditions: $V(\text{H}_2) / V(\text{CO}_2) = 4$, $T = 260$ °C, $P = 3.0$ MPa, $\text{GHSV} = 1500$ mL·g_{cat}⁻¹·h⁻¹.

3.4. H₂-TPR analysis of catalyst

H₂-TPR was used to analyze the effects of La₂O₃ and CeO₂ on the reduction properties of Cu–Fe–La and Cu–Fe–Ce catalysts, and the results are shown in Fig. 4.

The peak shape for the Cu–Fe–La catalyst is similar to that of the CuO–Fe₂O₃ catalyst, whereas the peak shape of the Cu–Fe–Ce catalyst differs from that of the CuO–Fe₂O₃ catalyst. Three Gaussian fitting peaks (α , β and γ) are shown for the Cu–Fe–La and Cu–Fe–Ce catalysts. In addition, the three reduction peaks (α , β and γ) correspond to the reduction process of highly dispersed CuO, small particles of CuO, and larger grains of bulk CuO, respectively [13,31]. The temperatures and areas of each reducing peak are summarized in Table 2.

The hydrogen reduction peaks (α), of the Cu–Fe–La and Cu–Fe–Ce catalysts are centered at 161 °C and 156 °C, respectively; these peaks were 16 °C and 11 °C lower than those of the CuO–Fe₂O₃ catalyst and 12 °C and 7 °C lower than those of the Cu–Fe–Zr catalyst. This indicated that the reducibility of highly dispersed CuO is enhanced by La and Ce modification. Cu is the active component in the catalytic hydrogenation of CO₂ to DME [32], and a lower reducing temperature will help to avoid

the sintering of the Cu active species and the formation of Cu crystal grains during the hydrogenation process. Furthermore, more Cu would be exposed on the surface of the catalyst, which could increase the reducibility of the catalyst [33,34]. The reduction properties of highly disperse CuO corresponding to peak α are closely related to the reduction properties of the Cu-based catalyst [35]; thus, modifying the CuO–Fe₂O₃ catalyst with La or Ce may improve the reducibility of the catalyst.

The temperature of peak α of the Cu–Fe–Ce catalyst was the lowest, suggesting that the Cu–Fe–Ce catalyst exhibited optimum reducing behavior. Moreover, the area of the reducing peaks α in the Cu–Fe–Ce catalyst was 20.9% higher than that in the Cu–Fe–La catalyst. At the same time, the areas of the reducing peaks α in Cu–Fe–La and Cu–Fe–Ce were 15.3% and 28.7% of the total area of the reducing peaks, respectively; the corresponding value for Cu–Fe was 7.77%. This results suggested that the proportion of highly disperse CuO was greatly increased by modifying with La and Ce. In addition, the total hydrogen consumption of Cu–Fe–Ce was decreased compared to that of the Cu–Fe catalyst. Considering the XRD results, this might be because CuO and CeO₂ formed a solid solution.

3.5. Catalytic hydrogenation of CO₂ to DME

The Cu–Fe–La/HZSM-5 and Cu–Fe–Ce/HZSM-5 bifunctional catalysts were used for the direct synthesis of DME from CO₂ and H₂. The catalytic activities of the two catalysts were compared with those of Cu–Fe/HZSM-5 and Cu–Fe–Zr/HZSM-5, and the results are shown in Table 3.

As shown in Table 3, the conversions of CO₂ and selectivity of DME were 12.3%, 17.3%, 17.2%, and 18.1% and 18.3%, 39.9%, 51.3%, and 52.0%. Compared with the Cu–Fe/HZSM-5 catalyst, the catalysts modified with ZrO₂, La₂O₃, and CeO₂ exhibited improved the CO₂ conversion and the DME selectivity along with reduced selectivity for CO and CH₄. These results suggest that ZrO₂, La₂O₃ and CeO₂ can improve the catalytic activity of the Cu–Fe catalyst in the catalytic hydrogenation of CO₂ to DME. Combined with the XPS and H₂-TPR results, modifying the Cu–Fe catalyst with Ce decreased the Cu outer-shell electron density and improved the reduction ability of Cu–Fe, which increased the CO₂ conversion and DME selectivity. Furthermore, the Cu–Fe–Ce catalyst has a greater specific surface area than the Cu–Fe–La catalyst. The Cu–Fe–Ce catalyst also promotes CuO dispersion and decreases CuO crystallite size. Thus, the catalytic activity (determined as the CO₂ conversion and DME selectivity) of the Cu–Fe–Ce catalyst is higher than that of Cu–Fe–La. When the Cu–Fe–Ce/HZSM-5 catalyst with 1.0 wt.% CeO₂ was used in the catalytic hydrogenation of CO₂ to DME at 260 °C and 3.0 MPa with $\text{GHSV} = 1500$ mL·g_{cat}⁻¹·h⁻¹, the CO₂ conversion was 18.1%, and the DME selectivity was 52.0%.

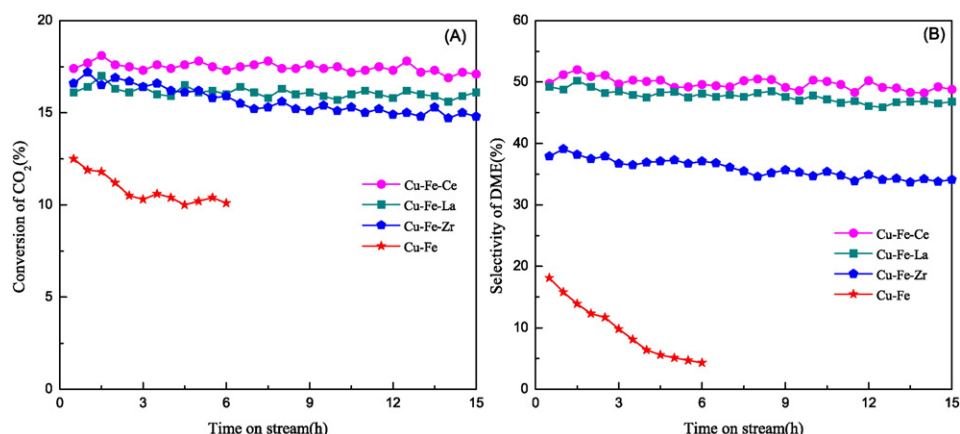


Fig. 5. Effects of the conversion of CO₂ (A) and the selectivity of DME (B) with Cu–Fe, Cu–Fe–Zr, Cu–Fe–La, Cu–Fe–Ce with time on stream.

3.6. The stabilities of the modified Cu–Fe/HZSM-5 catalysts

The stability of Cu–Fe/HZSM-5 and Cu–Fe/HZSM-5 modified with 1 wt.% Zr, La, and Ce were studied for the synthesis of DME via CO₂/H₂ at 260 °C and 3.0 Mpa, with GHSV = 1500 mL·g_{cat}⁻¹·h⁻¹ and V(H₂)/V(CO₂) = 4. The stabilities were recorded every 0.5 h and are shown in Fig. 5. During a 15-h reaction process, the CO₂ conversion and DME selectivities of the Ce- and La-modified Cu–Fe catalysts remained almost constant at 17.5% and 49.7%, 16.1% and 47.7%. The CO₂ conversion and DME selectivities of the Zr-modified Cu–Fe catalysts decreased from 16.6% to 14.8%, and from 36.5% to 34.1% with time on stream. However, the CO₂ conversion and DME selectivities of the Cu–Fe catalysts sharply declined with time on stream, indicating that the stabilities of the Cu–Fe catalyst modified with Zr, La, and Ce should be improved.

4. Conclusions

Cu–Fe–La and Cu–Fe–Ce catalysts were prepared via homogeneous precipitation. XRD revealed that the crystallite sizes of CuO in the CuO–Fe₂O₃ catalyst modified by La and Ce were 19.1 and 17.6 nm, respectively, and the reduction temperatures of highly dispersed CuO decreased by 16 and 11 °C, respectively, compared to that the CuO–Fe₂O₃ catalyst. Ce modifying decreased the Cu outer-shell electron density and improved the catalyst's reduction ability. The Cu–Fe–Ce catalyst had a greater specific surface area than the Cu–Fe–La catalyst and was able to promote CuO dispersion and decrease CuO crystallite size, indicating that the catalytic activity of the Cu–Fe–Ce catalyst was higher than that of Cu–Fe–La. Moreover, the Cu–Fe catalysts modified with La and Ce can improve catalyst stability. When the Cu–Fe–Ce/HZSM-5 catalyst with 1.0 wt.% CeO₂ was used in the catalytic hydrogenation of CO₂ to DME at 260 °C and 3.0 MPa with GHSV = 1500 mL·g_{cat}⁻¹·h⁻¹, the CO₂ conversion was 18.1%, the DME selectivity was 52.0%, and the catalyst was stable for 15 h.

Acknowledgments

This work was supported by National Natural Science Foundation of China (21366004, 21425627), Guangxi Zhuang Autonomous Region special funding of distinguished experts, and Open Project of Guangxi Key Laboratory of Petrochemical Resource Processing and Process Intensification Technology.

References

- [1] P. Cox, C. Jones, Illuminating the modern dance of climate and CO₂, *Science* 321 (2008) 1642–1644.
- [2] G. Centi, S. Perathoner, Opportunities and prospects in the chemical recycling of carbon dioxide to fuels, *Catal. Today* 148 (2009) 191–205.
- [3] Z. Jiang, T. Xiao, V.L. Kuznetsov, P.P. Edwards, Turning carbon dioxide into fuel, *Philos. Trans. R. Soc. London, Ser. A* 368 (2010) 3343–3364.
- [4] G.A. Olah, A. Goepfert, G.K.S. Prakash, Chemical recycling of carbon dioxide to methanol and dimethyl ether: from greenhouse gas to renewable, environmentally carbon neutral fuels and synthetic hydrocarbons, *J. Org. Chem.* 74 (2009) 487–498.
- [5] S. Wang, D. Mao, X. Guo, G. Wu, G. Lu, Dimethyl ether synthesis via CO₂ hydrogenation over CuO–TiO₂–ZrO₂/HZSM-5 bifunctional catalysts, *Catal. Commun.* 10 (2009) 1367–1370.
- [6] H. Ahouari, A. Soualah, A. Le Valant, L. Pinard, P. Magnoux, Y. Pouilloux, Methanol synthesis from CO₂ hydrogenation over copper based catalysts, *React. Kinet. Mech. Catal.* 110 (2013) 131–145.
- [7] R. Liu, H. Tian, A. Yang, F. Zha, J. Ding, Y. Chang, Preparation of HZSM-5 membrane packed CuO–ZnO–Al₂O₃ nanoparticles for catalysing carbon dioxide hydrogenation to dimethyl ether, *Appl. Surf. Sci.* 345 (2015) 1–9.
- [8] F. Frusteri, M. Cordaro, C. Cannilla, G. Bonura, Multifunctionality of Cu–ZnO–ZrO₂/HZSM5 catalysts for the one-step CO₂-to-DME hydrogenation reaction, *Appl. Catal. B Environ.* 162 (2015) 57–65.
- [9] L. Bie, H. Wang, W. Gao, C. Wang, Hybrid catalysts for the direct synthesis of dimethyl ether from carbon dioxide hydrogenation in a slurry reactor, *Chem. Ind. Eng. Prog.* 28 (2009) 1365–1370 (In Chinese).
- [10] F. Frusteri, G. Bonura, C. Cannilla, G. Drago Ferrante, A. Aloise, E. Catizzone, M. Migliori, G. Giordano, Stepwise tuning of metal-oxide and acid sites of CuZnZr-

- MFI hybrid catalysts for the direct DME synthesis by CO₂ hydrogenation, *Appl. Catal. B Environ.* 176–177 (2015) 522–531.
- [11] O. Oyola-Rivera, M.A. Baltanás, N. Cardona-Martínez, CO₂ hydrogenation to methanol and dimethyl ether by Pd–Pd₂Ga catalysts supported over Ga₂O₃ polymorphs, *J. CO₂ Util.* 9 (2015) 8–15.
- [12] L. Li, B. Zhang, E. Kunkes, K. Föttinger, M. Armbrüster, D.S. Su, W. Wei, R. Schlögl, M. Behrens, Ga–Pd/Ga₂O₃ catalysts: the role of Gallia polymorphs, intermetallic compounds, and pretreatment conditions on selectivity and stability in different reactions, *ChemCatChem* 4 (2012) 1764–1775.
- [13] R.-w. Liu, Z.-z. Qin, H.-b. Ji, T.-m. Su, Synthesis of dimethyl ether from CO₂ and H₂ using a Cu–Fe–Zr/HZSM-5 catalyst system, *Ind. Eng. Chem. Res.* 52 (2013) 16648–16655.
- [14] Z.-z. Qin, T.-m. Su, H.-b. Ji, Y.-x. Jiang, R.-w. Liu, J.-h. Chen, Experimental and theoretical study of the intrinsic kinetics for dimethyl ether synthesis from CO₂ over Cu–Fe–Zr/HZSM-5, *AIChE J.* 61 (2015) 1613–1627.
- [15] W. Li, X. Yu, Research progress in dimethyl ether synthesis by hydrogenation of carbon dioxide, *Nat. Gas Chem. Ind.* 34 (2009) 59–62 (in Chinese).
- [16] W. Gao, H. Wang, Y. Wang, W. Guo, M. Jia, Dimethyl ether synthesis from CO₂ hydrogenation on La-modified CuO–ZnO–Al₂O₃/HZSM-5 bifunctional catalysts, *J. Rare Earths* 31 (2013) 470–476.
- [17] S. Wang, L. Zhao, W. Wang, Y. Zhao, G. Zhang, X. Ma, J. Gong, Morphology control of ceria nanocrystals for catalytic conversion of CO₂ with methanol, *Nanoscale* 5 (2013) 5582–5588.
- [18] I. Prymak, V.N. Kalevaru, S. Wohlrab, A. Martin, Continuous synthesis of diethyl carbonate from ethanol and CO₂ over Ce–Zr–O catalysts, *Catal. Sci. Technol.* 5 (2015) 2322–2331.
- [19] L. Zhang, L. Pan, C. Ni, T. Sun, S. Zhao, S. Wang, A. Wang, Y. Hu, CeO₂–ZrO₂-promoted CuO/ZnO catalyst for methanol steam reforming, *Int. J. Hydrog. Energy* 38 (2013) 4397–4406.
- [20] Y. Liu, T. Hayakawa, K. Suzuki, S. Hamakawa, T. Tsunoda, T. Ishii, M. Kumagai, Highly active copper/ceria catalysts for steam reforming of methanol, *Appl. Catal. A Gen.* 223 (2002) 137–145.
- [21] L. Samiee, F. Shoghi, A. Vinu, Fabrication and electrocatalytic application of functionalized nanoporous carbon material with different transition metal oxides, *Appl. Surf. Sci.* 265 (2013) 214–221.
- [22] W. Zhan, Y. Guo, X. Gong, Y. Guo, Y. Wang, G. Lu, Surface oxygen activation on CeO₂ and its catalytic performances for oxidation reactions, *Sci. Sin. Chim.* 42 (2012) 433–445.
- [23] J.P. Espinós, J. Morales, A. Barranco, A. Caballero, J.P. Holgado, A.R. González-Elipé, Interface effects for Cu, CuO, and Cu₂O deposited on SiO₂ and ZrO₂, XPS determination of the valence state of copper in Cu/SiO₂ and Cu/ZrO₂ catalysts, *J. Phys. Chem. B* 106 (2002) 6921–6929.
- [24] S.D. Jones, L.M. Neal, M.L. Everett, G.B. Hoflund, H.E. Hagelin-Weaver, Characterization of ZrO₂-promoted Cu/ZnO/nano-Al₂O₃ methanol steam reforming catalysts, *Appl. Surf. Sci.* 256 (2010) 7345–7353.
- [25] A.P. Grosvenor, B.A. Kobe, M.C. Biesinger, N.S. McIntyre, Investigation of multiplet splitting of Fe 2p XPS spectra and bonding in iron compounds, *Surf. Interface Anal.* 36 (2004) 1564–1574.
- [26] M.F. Sunding, K. Hadidi, S. Diplas, O.M. Løvvik, T.E. Norby, A.E. Gunnæs, XPS characterisation of in situ treated lanthanum oxide and hydroxide using tailored charge referencing and peak fitting procedures, *J. Electron Spectrosc. Relat. Phenom.* 184 (2011) 399–409.
- [27] J. Silvestre-Albergo, F. Rodríguez-Reinoso, A.A. Sepúlveda-Escribano, Improved metal-support interaction in Pt/CeO₂/SiO₂ catalysts after zinc addition, *J. Catal.* 210 (2002) 127–136.
- [28] E. Moretti, L. Storaro, A. Talon, M. Lenarda, P. Riello, R. Frattini, M.d.V.M. de Yuso, A. Jiménez-López, E. Rodríguez-Castellón, F. Ternero, A. Caballero, J.P. Holgado, Effect of thermal treatments on the catalytic behaviour in the CO preferential oxidation of a CuO–CeO₂–ZrO₂ catalyst with a flower-like morphology, *Appl. Catal. B Environ.* 102 (2011) 627–637.
- [29] S. Zeng, Y. Wang, K. Liu, F. Liu, H. Su, CeO₂ nanoparticles supported on CuO with petal-like and sphere-flower morphologies for preferential CO oxidation, *Int. J. Hydrog. Energy* 37 (2012) 11640–11649.
- [30] F. Tonelli, O. Gorzic, A. Tarditi, L. Cornaglia, L. Arrúa, M. Cristina Abello, Activity and stability of a CuO/CeO₂ catalyst for methanol steam reforming, *Int. J. Hydrog. Energy* 40 (2015) 13379–13387.
- [31] Y. Zhou, S. Wang, M. Xiao, D. Han, Y. Lu, Y. Meng, Novel Cu–Fe bimetal catalyst for the formation of dimethyl carbonate from carbon dioxide and methanol, *RSC Adv.* 2 (2012) 6831–6837.
- [32] H. Nakatsujii, Z.-M. Hu, Mechanism of methanol synthesis on Cu(100) and Zn/Cu(100) surfaces: comparative dipped adcluster model study, *Int. J. Quantum Chem.* 77 (2000) 341–349.
- [33] M.-H. Zhang, Z.-M. Liu, G.-D. Lin, H.-B. Zhang, Pd/CNT-promoted CuZrO₂/HZSM-5 hybrid catalysts for direct synthesis of DME from CO₂/H₂, *Appl. Catal. A Gen.* 451 (2013) 28–35.
- [34] R. Khoshbin, M. Haghghi, Direct syngas to DME as a clean fuel: the beneficial use of ultrasound for the preparation of CuO–ZnO–Al₂O₃/HZSM-5 nanocatalyst, *Chem. Eng. Res. Des.* 91 (2013) 1111–1122.
- [35] Z. Li, J. Li, M. Dai, Y. Liu, D. Han, J. Wu, The effect of preparation method of the Cu–La₂O₃–ZrO₂/γ-Al₂O₃ hybrid catalysts on one-step synthesis of dimethyl ether from syngas, *Fuel* 121 (2014) 173–177.